Metal-binding affinity of a series of bis-benzimidazoles immobilised on silica

Hans J. Hoorn,[a] Peter de Joode,[a] Dirk J. Dijkstra,[a] Willem L. Driessen,*[a] Huub Kooijman,[b] Nora Veldman,[b] Anthony L. Spek[b] and Jan Reedijk[a]

[a]*Leiden Institute of Chemistry, Gorlaeus Laboratories, Leiden University, P.O. Box 9502, 2300 RA Leiden, The Netherlands*

[b]*Bijvoet Center for Biomolecular Research, Crystal and Structural Chemistry, Utrecht University, Padualaan 8, 3584 CH Utrecht, The Netherlands*

Three potentially tridentate bis(benzimidazol-2-ylalkyl)amines have been immobilised on silica *via* the bifunctional spacer (3-glycidoxypropyl)trimethoxysilane (GLYMO). The obtained ligand concentrations are in the range 0.53–0.66 mmol/g ion exchanger. These ion exchangers selectively adsorb Cu^{2+}, with a maximum capacity in the range 0.29–0.47 mmol g^{-1} at pH 5.6 from aqueous solutions, containing a mixture of the divalent metal ions Cu^{2+}, Ni^{2+}, Co^{2+}, Cd^{2+} and Zn^{2+}. Strong binding of Cu^{2+}, even at a pH as low as 1, was observed with Alfa-BBAH showing that coordination *via* a five-membered chelate is favoured over a six-membered chelate as in the case of Alfa-BBEAH. Although, potentially, two different didentate coordination modes are possible with Alfa-BBPAH (*i.e.* through five- and seven-membered chelate structures), the Cu^{2+} uptake and distribution coefficients show a high similarity with Alfa-BBAH, suggesting strong chelation *via* the stable five-membered chelate. The coordination chemistry of the ligand BBPAH is further illustrated by the presentation of the crystal structures with the reference compounds $CuCl_2$ and $Ni(NO_3)_2$. Fast uptake and regeneration kinetics were found with these ion exchangers, but complete regeneration of Alfa-BBAH takes significantly longer than for the other two. With Alfa-BBAH and Alfa-BBEAH a significant reduction of the capacity is seen after several cycles of consecutive loading and regeneration which was shown to be caused by hydrolysis of the siloxane bond of the silica surface.

Ion exchange has been widely studied for the recovery of metals in water treatment. Where it is desirable to recover metals in a pure form, few economic options are available. A wide variety of techniques have been developed for the separation of a wide range of mixtures of different metal ions. Considerable effort has been focused on scaling batch processes to an industrial scale.[1] To allow expansion of the use of the technology in industry, it has been necessary to achieve continuous operation. This has resulted in the development of new techniques, like membrane-assisted separation processes, based on small ion-exchange particles.[2,3] The efficiency of these processes is strongly determined by the ion-exchange particles used. Most commercial ion-exchange resins show high capacities but often suffer from low selectivity and slow kinetics.[4,5] To improve selectivity and kinetics, small chemically modified silica particles have been used in the present study. Chemically modified silicas are easily accessible and have been used in a variety of chromatographic applications.[6–8]

A ligand can be immobilised onto a silica surface *via* a bifunctional spacer like (3-glycidoxypropyl)trimethoxysilane (GLYMO). The epoxide group is known to react with a variety of nucleophiles by ring opening.[9] Through the reaction of a siloxane with the surface silanol groups, a relatively stable linkage can be formed.[10] The present paper reports the immobilisation of a series of potentially tridentate bis(benzimidazol-2-ylalkyl)amines, selected to study the effect of the structure of the ligand on the metal-uptake characteristics. The results are compared with results obtained with these ligands immobolised on different kinds of resins.[11,5,12*a*]

Experimental

Starting materials

All reagents and solvents were purchased from commercial sources and used without further purification. Silica (Alfa, large pore, surface area 450 m^2 g^{-1}, particle size <2 μm, pore volume 1.6 ml g^{-1}) was activated before use by heating *in vacuo* at 150 °C for 48 h.

Analyses

Elemental analyses (C,H,N) were performed by the Microanalytical department of Groningen University (The Netherlands). Metal analyses were carried out on a Perkin-Elmer 3100 atomic absorption (AAS) and flame emission spectrometer connected to a Perkin-Elmer AS-90 autosampler using a non-linear calibration method.

Spectroscopic methods

^1H and ^{13}C NMR spectra were recorded on a JEOL JNM FT-NMR spectrometer connected to a Macintosh Iivx computer. Chemical shifts are reported with respect to TMS as internal reference. ^{13}C MAS NMR spectra (cross-polarisation magic angle spinning) were recorded on a Bruker MSL 400 spectrometer, operating at 400.1 and 100.6 MHz for ^1H and ^{13}C, respectively. The used sample spinning rate was 7000 Hz for ^{13}C. The cross-polarisation contact time was 1.0 ms with 3 s recycle delays between successive scans. Generally 18 000 to 64 000 scans were employed. Solid-state electronic spectra (28 000–5000 cm^{-1}), using the diffuse reflectance method with dried zinc(II)-loaded samples as a reference, were recorded on a Perkin-Elmer 330 spectrophotometer equipped with a data station. Electron paramagnetic resonance (EPR) spectra were recorded on a JEOL JES-RE2X ESR spectrophotometer equipped with a JEOL Esprit 330 data system at X-band frequencies, using DPPH ($g=2.0036$) as a reference.

Batch metal-uptake experiments

The batch metal-uptake experiments were performed using standard metal chloride solutions of 0.16 M with 0.6 M buffer solutions NaCl–HCl (pH 1.1–2.0) and NaOAc–HOAc (pH 2.5–6.0). All experiments were performed in polyethylene bottles mounted on a shaker at room temperature.

The capacities for Cu^{2+}, Ni^{2+}, Cd^{2+}, Co^{2+}, Zn^{2+} and Ca^{2+} under non-competitive conditions were determined in a pH range from 1 to 6.0. Batches of 0.2 g ion-exchange material were used, together with a mixture of 25 ml of metal solution and 25 ml of acid or buffer. After a shaking time of 48 h, the samples were filtered off, washed with water, ethanol and diethyl ether, respectively, and dried *in vacuo* at 50 °C. For the determination of the Cu^{2+} capacities at pH > 5 a lower Cu^{2+} concentration (12.5 ml of the standard Cu^{2+} solution, 12.5 ml demineralised water and 25 ml of buffer) was used to prevent precipitation of $Cu(OH)_2$.

Batch metal-uptake experiments under competitive conditions were performed with standard metal chloride solutions of Cu^{2+}, Ni^{2+}, Cd^{2+}, Co^{2+} and Zn^{2+} in a pH range from 1 to 6.0. Batches of 0.2 g ion-exchange material were used together with a mixture of 5 ml of each metal solution and 25 ml of acid or buffer. After a shaking time of 48 h, the samples were further handled as described for the non-competitive experiments.

For the determination of the metal-uptake kinetics, 0.1 g of ion-exchanger material was soaked with 2 ml buffer (pH 5.0) in test tubes for 1 min. Then 2 ml of the standard $CuCl_2$ solution was added to each sample. The test tubes were mixed on a vortex mixer for 5 s, 15 s, 30 s, 60 s, 2 min, 5 min, 15 min, 30 min, 1 h, 24 h and 48 h, respectively. The samples were further handled as described for the non-competitive experiments.

For the determination of the stripping kinetics, 0.1 g of Cu^{2+}-loaded (pH 5.0) ion-exchange material in a test tube was contacted with 4 ml 0.5 M H_2SO_4. The test tubes were mixed on a vortex mixer for 5 s, 15 s, 30 s, 60 s, 2 min, 15 min, 30 min, 1 h, 24 h and 48 h, respectively. The samples were further handled as described for the non-competitive experiments.

In the regeneration experiments, batches of the ion-exchange materials (each 1.0 g) were loaded with a $CuCl_2$ solution (25 ml of the metal standard solution and 25 ml of HOAc–NaOAc buffer pH 4.5) by shaking for a period of 24 h. The loaded samples were stripped with a 0.5 M H_2SO_4 solution (shaking time 24 h). These procedures were repeated four times with fresh solutions.

For the determination of the kinetic selectivity under competitive conditions, 0.1 g ion-exchange material in a test tube was soaked with 2 ml buffer (pH 5.0). Then 2 ml 1 : 1 mixture of standard $CuCl_2$ solution with standard $ZnCl_2$ solution was added. The test tubes were mixed on a vortex mixer for 5 s, 15 s, 30 s, 60 s, 2 min, 5 min, 15 min, 30 min, 1 h, 24 h and 48 h, respectively. The samples were further handled as described for the non-competitive experiments.

Samples for metal analysis were prepared by heating 0.1 g of the loaded samples with concentrated H_2SO_4 for 24 h and subsequently with concentrated HNO_3, until clear solutions were obtained. The metal contents of these solutions were measured by AAS spectroscopy using a non-linear calibration curve. The capacities, determined *via* this batch method, were corrected for the increase in mass caused by the amount of metal and anion adsorbed.

For the distribution coefficients, batches of ion-exchanger material equivalent to 0.13 mmol ligand were loaded with 25 ml 1.0 mmol Cu^{2+} l^{-1} and 25 ml buffer in the pH range 1.1–6.0. After shaking for 48 h, 5 ml of supernatant was transferred into a 50 ml volumetric flask. The samples were filtered off quantitatively, washed with water, ethanol and heated with H_2SO_4 for 24 h and subsequently with concentrated HNO_3, until clear solutions were obtained. The metal contents of the supernatant and the residue were measured by atomic absorption spectroscopy, using a non-linear calibration curve.

To obtain information about the coordination environment of the metal ions bound to the ion-exchange materials, electronic spectra in the visible and near infrared (VIS–NIR) and EPR spectra of several loaded ion-exchange materials were recorded. Batches of *ca.* 0.2 g were treated with aqueous solutions of MCl_2 as described for the capacity experiments. Dried Cu^{2+}-loaded samples were used for EPR spectroscopy at room temperature.

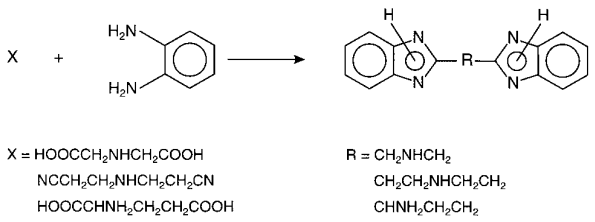

Scheme 1 Schematic representation of the synthesis of the bis(benzimidazol-2-ylalkyl)amines

Synthesis of the ligands

The synthesis of the ligands is as shown in Scheme 1. Synthesis of *N*,*N*′-bis(benzimidazol-2-ylmethyl)amine (BBAH), and 1,3-bis(benzimidazol-2-yl)propylamine (BBPAH) were performed according to literature procedures.[12] *N*,*N*′-Bis(benzimidazol-2-ylethyl)amine (BBEAH) was synthesised by a modified procedure of the synthesis described by Sorrell and Garrity.[13]

3,3′-Iminopropionitrile (80% solution) (15 g, 0.097 mmol) and 1,2-diaminobenzene (20.6 g, 0.19 mol) were refluxed for four days in 6 M hydrochloric acid (250 ml). Water (200 ml) was added and the solution was cooled in an ice–water mixture. Ammonia (33%) was carefully added under vigorous stirring until pH 8. The precipitate was filtered off and washed with water. The residue was dissolved in methanol and refluxed with active carbon. The mixture was filtered and water was added. The white precipitate was collected and dried *in vacuo* at 50 °C. Yield BBEAH, 20 g (69%). ^{1}H NMR (CD_3OD): δ 3.26 (m, 4H, CH_2NH), 3.55 (t, 4H, CH_2), 7.10 [m, 4H, benzimidazole C(4/7)], 7.30 [m, 4H, benzimidazole C(5/6)]. ^{13}C NMR (CD_3OD): δ 28.0 (CH_2CH_2NH), 47.4 (CH_2NH), 115.5 [benzimidazole C(4/7)], 123.4 [benzimidazole C(5/6)], 139.4 [benzimidazole C(8/9)], 153.6 [benzimidazole C(2)].

Preparation and characterisation of the ion exchangers

The synthesis of the ion-exchange materials is shown in Scheme 2. The ligand (42 mmol) and GLYMO (9.9 g, 42 mmol) were dissolved in dry methanol (150 ml). The mixture was refluxed under a dinitrogen atmosphere for 65 h. The solution was concentrated to approximately 50 ml and added to 18 g silica in dry toluene (400 ml). After refluxing for 48 h under a dinitrogen atmosphere, the reaction mixture was evaporated to dryness and the residue was dried at 50 °C *in vacuo* for 24 h. The product was extracted with methanol in a Soxhlet apparatus during 10 h. The product was dried at 50 °C *in vacuo* for 24 h. The products, Alfa-BBAH (**1**), Alfa-BBEAH (**2**) and Alfa-BBPAH (**3**) were off-white in colour.

Alfa-GLYMO was synthesised by refluxing GLYMO (7.1 g, 30 mmol) with 10 g of silica in dry toluene (250 ml) for 24 h. The reaction mixture was evaporated to dryness and dried at 50 °C *in vacuo* for 24 h. The product was extracted with methanol, using a Soxhlet apparatus during 10 h, and dried at 50 °C *in vacuo* for 24 h. Alfa-GLYMO was used as a reference for spectroscopic measurements.

Preparation of the coordination compounds

The coordination compounds with 1,3-bis(benzimidazol-2-yl)propylamine (BBPAH), $[Cu(BBPAH)(EtOH)(Cl)]_nCl_n$ and $[Ni(BBPAH)(H_2O)(NO_3)]NO_3{\cdot}2EtOH$, were prepared by dissolving 2 mmol $CuCl_2{\cdot}2H_2O$ or $Ni(NO_3)_2{\cdot}6H_2O$ in a hot mixture of 100% ethanol (20 ml) and triethylorthoformate (4 ml). To this mixture, a solution of 2 mmol BBPAH in hot

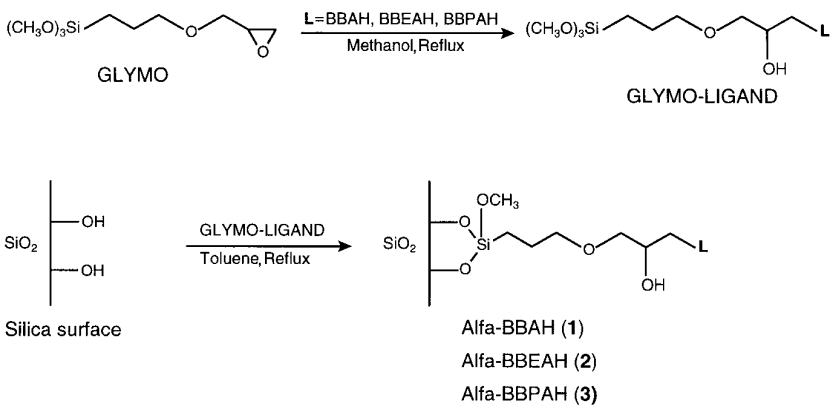

Scheme 2 Immobilisation of the bis-benzimidazoles on the silica support

ethanol (20 ml) was added. After filtration of the reaction mixture, the complexes crystallised upon slow evaporation of the solvent.

Single-crystal structure determinations

Crystal data for [Cu(BBPAH)(EtOH)(Cl)]$_n$Cl$_n$·(*n*/2) C_2H_6O. $C_{19}H_{23}Cl_2CuN_5O{\cdot}0.5C_2H_6O$, $M_r = 494.91$, blue, rod-shaped crystal ($0.1 \times 0.2 \times 0.5$ mm), orthorhombic, space group *Pbca* (no. 61) with $a = 11.667(2)$, $b = 16.144(2)$, $c = 24.531(3)$ Å, $V = 4620.5(11)$ Å^3, $Z = 8$, $D_c = 1.423$ g cm^{-3}, $F(000) = 2048$, μ(Mo-Kα) = 12.0 cm^{-1}. 6563 Reflections measured, 5265 independent ($0.83° < \theta < 27.50°$, ω–2θ scan, $T = 150$ K, Mo-Kα radiation, graphite monochromator, $\lambda = 0.710\,73$ Å) on an Enraf-Nonius CAD4 Turbo diffractometer on rotating anode. Data were corrected for L_p effects and for linear instability of the reference reflections during X-ray exposure time; no absorption correction applied. The structure was solved by automated Patterson methods (DIRDIF92).[14] Refinement on F^2 was carried out by full-matrix least-squares techniques (SHELXL-93);[15] no observance criterion was applied during refinement. Atom C(2) displays conformational disorder; the non-coordinated ethanol molecule is disordered over a crystallographic inversion centre. Hydrogen atoms were included in the refinement on calculated positions riding on their carrier atoms. All non-hydrogen atoms, except those involved in disorder models were refined with anisotropic thermal parameters. Hydrogen atoms were refined with a fixed isotropic displacement parameter related to the value of the equivalent isotropic displacement parameter of their carrier atoms. Refinement converged at $wR_2 = \sum w(F_o^2 - F_c^2)^2]/\sum[w(F_o^2)^2]]^{1/2} = 0.219$, $R_1 = \sum||F_o| - |F_c||/\sum|F_o| = 0.091$ [for 2175 reflections with $I > 2\sigma(I)$], $S = 0.95$, for 269 parameters. A final difference Fourier mass showed no residual density outside -0.59 and 0.68 e Å^{-3}.

Crystal data for [Ni(BBPAH)(H$_2$O)(NO$_3$)]NO$_3$·2EtOH. The general procedure described above was adopted. Pertinent data are as follows: $C_{17}H_{19}N_7NiO_7{\cdot}2C_2H_6O$, $M_r = 584.21$, blue, block-shaped crystal ($0.25 \times 0.45 \times 0.63$ mm), orthorhombic, space group *Pbca* (no. 61) with $a = 11.280(3)$, $b = 17.416(3)$, $c = 26\,697(3)$ Å, $V = 5244.7(18)$ Å^3, $Z = 8$, $D_c = 1.480$ g cm^{-3}, $F(000) = 2448$, μ(Mo-Kα) = 8.0 cm^{-1}. 5156 Reflections measured, 4598 independent included in structure determination, (ω scan, $0.76° < \theta < 25.00°$). An empirical absorption correction was applied (DIFABS).[16] Refinement converged at $wR_2 = 0.225$, $R_1 = 0.093$ [for 2390 reflections with $I > 2\sigma(I)$], $S = 1.04$, for 359 parameters. A final difference Fourier showed no residual density outside -0.52 and 0.55 e Å^{-3}.

Atomic coordinates, thermal parameters, and bond lengths and angles for both compounds have been deposited at the Cambridge Crystallographic Data Centre (CCDC). See Information for Authors, *J. Mater. Chem.*, 1997, Issue 1. Any request to the CCDC for this material should quote the full literature citation and the reference number 1145/41.

Results and Discussion

Characterisation of the low-molecular-mass compounds

The numbering of the carbon atoms is shown in Scheme 3. The data are listed in Table 1. The C(6) and C(7) of GLYMO have shifted, on average, from δ 51.8 and 44.6 to δ 71 and 52, respectively, after reaction with BBAH, BBEAH and BBPAH. Their relative positions show that the amines have reacted at the C(7) position of GLYMO. All products show characteristic benzimidazole peaks around δ 115 [benzimidazole C(4/7)], 123 [benzimidazole C(5/6)], 139 [benzimidazole C(8/9)] and 154 [benzimidazole C(2)].

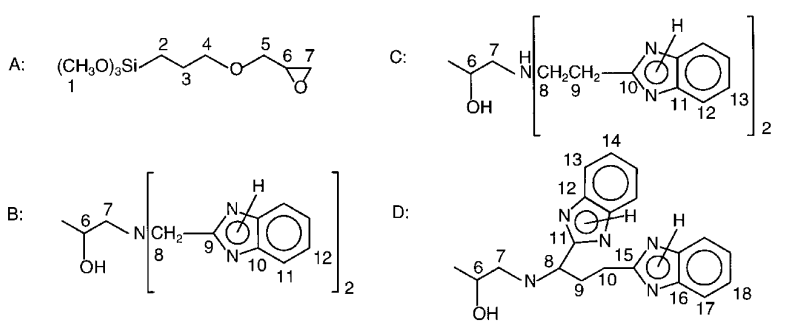

Scheme 3 Numbering scheme of compounds used for ^{13}C NMR; A, GLYMO; B, GLYMO-BBAH; C, GLYMO-BBEAH; D, GLYMO-BBPAH

Table 1 Tentative ^{13}C NMR chemical shift assignments. Chemical shifts are reported relative to TMS. The numbering of the carbon atoms is shown in Scheme 3

	δ (^{13}C) in solution				δ (^{13}C) in CP MAS			
	GLYMO[a]	GLYMO BBAH[b]	GLYMO BBEAH[a]	GLYMO BBPAH[b]	Alfa-GLYMO	**1**	**2**	**3**
C(1)	50.8	—[c]	47.5	50.4	50.6	50	52	51
C(2)	6.0	6.2	6.9	5.2	9.0	8	9	9
C(3)	23.9	23.9	23.9	22.6	22.9	23	24	23
C(4)	74.2	73.2	72.7	73.2	73.1	72	72	73
C(5)	72.7	74.4	74.1	73.2	71.7	72	72	73
C(6)	51.8	70.1	71.0	71.3	50.6	72	72	73
C(7)	44.6	54.3	52.3	49.8	43.6	50	52	51
C(8)		59.8	46.8	50.0		50	42	51
C(9)		154	29.4	25.5		152	24	23
C(10)		139.5	152.4	35.7		134	150	35
C(11)		115.7	138.9	156.8		110	133	155
C(12)		123.4	115.3	138.2		121	109	134
C(13)			123.1	114.9			122	111
C(14)				122.3				122
C(15)				154.5				155
C(16)				138.2				134
C(17)				114.5				111
C(18)				122.1				122

[a]In $CDCl_3$. [b]In CD_3OD. [c]Obscured by solvent peaks.

Elemental analysis

Results of the elemental analysis of the ion exchangers are listed in Table 2. Calculation of the ligand concentrations is based on the nitrogen contents found in the elemental analysis. Relatively high ligand concentrations are achieved, despite the fact that the ligands are much bulkier than the didentate analogs described in an earlier investigation.[17] This suggests that steric crowding at the silica surface is minimal.

^{13}C Solid-state NMR

CP MAS spectra are shown in Fig. 1 and data are listed in Table 1. The spectrum of GLYMO has been discussed previously and is redrawn for comparison purposes.[18] The spectra of ion exchangers **1**, **2** and **3** are very similar and show characteristic benzimidazole peaks in the range δ 150–155 [benzimidazole C(2)], 133–134 [benzimidazole C(8/9)], 121–122 [benzimidazole C(5/6)], 109–111 [benzimidazole C(4/7)].[19] Rather broad signals are observed in the aliphatic region making precise assignment difficult.

Metal uptake experiments

The metal capacities of ion exchangers **1**, **2** and **3** were measured under non-competitive conditions as a function of pH for Cu^{2+}, Ni^{2+}, Cd^{2+}, Co^{2+}, Zn^{2+} and Ca^{2+}. The ligand occupation was also calculated in order to have a more appropriate basis for the comparison of the ion-exchange materials.[17] The results are shown in Fig. 2. Ion exchanger **1** appears favourable for Cu^{2+}, Zn^{2+} and Cd^{2+} which is reflected by the relatively high ligand occupation for these metal ions over the whole pH range tested. The high uptake of Cd^{2+} and Zn^{2+} can be explained by their preferred formation of tetrahedral complexes with nitrogen-containing ligands.[20] The chelating properties of BBAH seem to be extra favourable, compared to BBEAH, probably caused by strong tridentate coordination by the nitrogen atoms. The capacity for Cu^{2+} is high even at pH 1, which indicates that protonation of the ligand is prevented through very strong coordination to Cu^{2+}. Ion exchanger **2** shows a more pH-dependent uptake of the metal ions and a lower ligand occupation is achieved than with ion exchanger **1**. The lower ligand occupation is probably caused by less favourable coordination of the more bulky ligand BBEAH around the metal ions. This less favourable binding causes easier protonation of the ligand and thus a more pH-dependent metal uptake is found. Ion exchanger **3** shows a high ligand occupation for Cu^{2+}, Zn^{2+} and Cd^{2+} at pH > 3. The ligand occupation by Cu^{2+} is hardly influenced by changes in pH which implies strong bonding of the ligand.

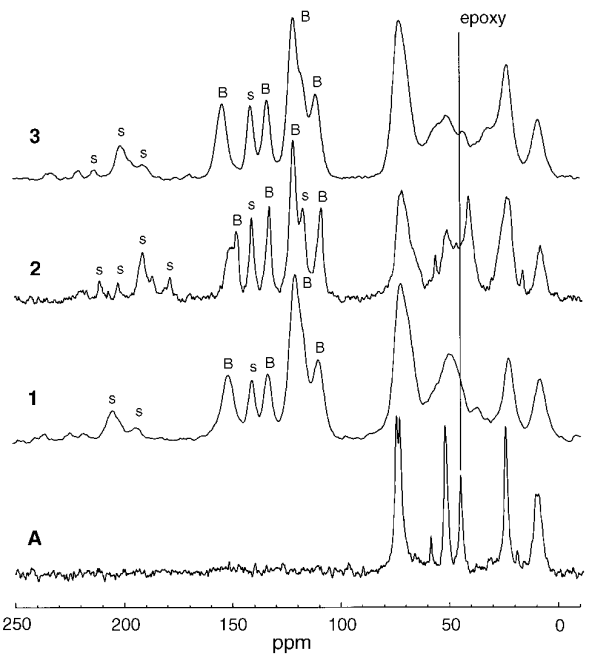

Fig. 1 ^{13}C CP MAS NMR spectra of A, Alfa-GLYMO (18 845 FIDs collected); **1**, Alfa-BBAH (28 065 FIDs collected); **2**, Alfa-BBEAH (18 383 FIDs collected); **3**, Alfa-BBPAH (64 000 FIDs collected). S denotes a side band, B denotes benzimidazole peak.

Table 2 Elemental analysis of the silica products

ion exchanger	C(%)	H(%)	N(%)	ligand concentration/ mmol g^{-1}
1	17.48	2.52	3.69	0.53
2	24.63	3.02	4.60	0.66
3	19.99	2.55	4.41	0.63

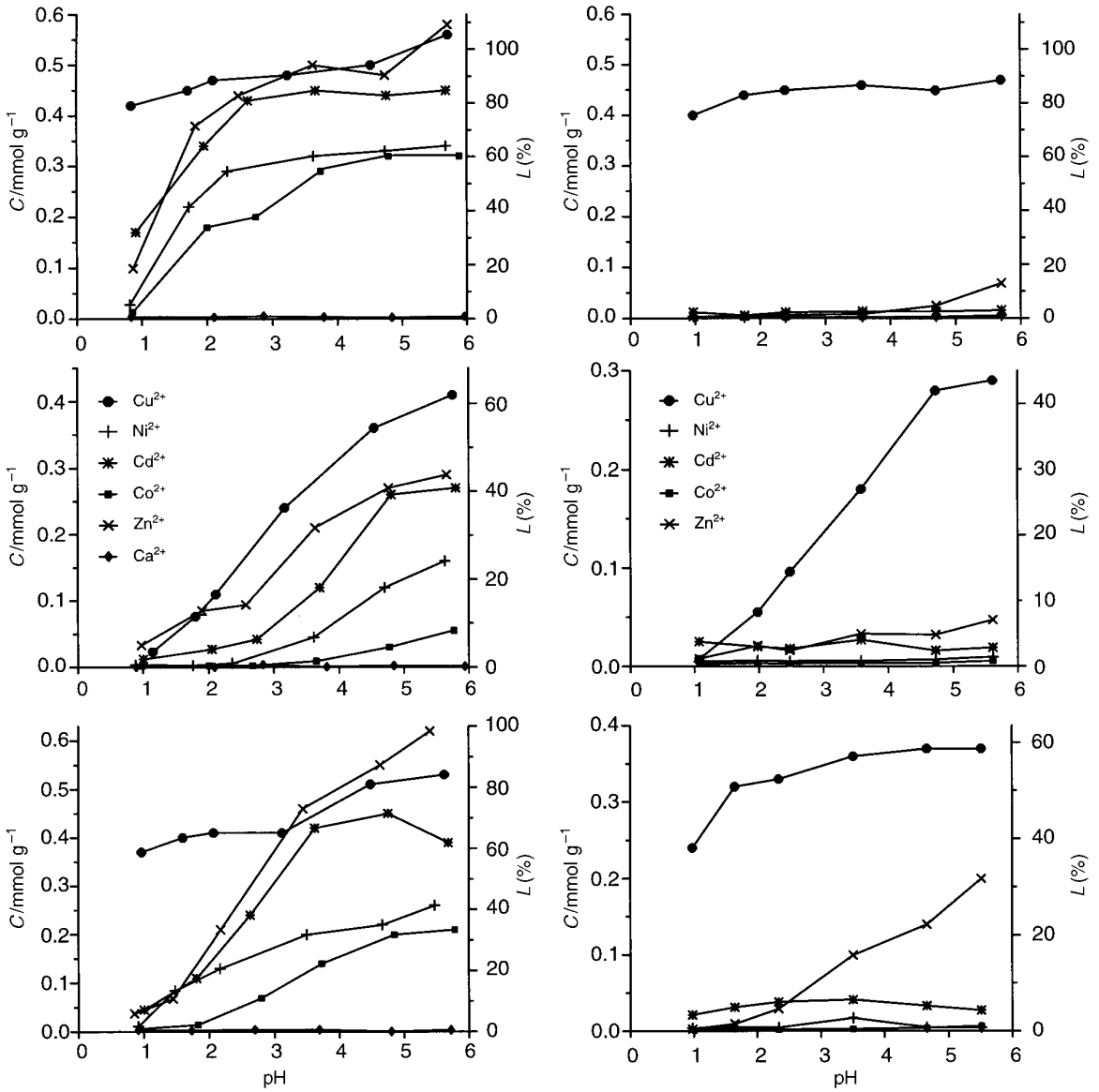

Fig. 2 Capacity (C) and ligand occupation (L) of ion exchangers **1** (upper), **2** (middle) and **3** (lower graphs) for the divalent metal ions as a function of pH under non-competitive conditions (left column) and under competitive conditions (right column) [Cu^{2+} ●, Ni^{2+} +, Cd^{2+} ✳, Co^{2+} ■, Zn^{2+} ×, Ca^{2+} ◆]

The coordination most likely occurs through the aliphatic amine and the 1-benzimidazole group to form a very stable five-membered chelate complex. The uptake of Zn^{2+} and Cd^{2+} is probably predominately through distorted tridentate coordination of the ligand in which the second benzimidazole group may be loosely coordinated. All ion exchangers show no significant uptake of Ca^{2+}. The metal-uptake pattern of these silica-based ion exchangers is very similar to those observed for polymer-based ion exchangers.[5,11,12a]

The metal capacities of ion exchangers **1**, **2** and **3** were measured under competitive conditions as a function of pH for Cu^{2+}, Ni^{2+}, Cd^{2+}, Co^{2+} and Zn^{2+} (Fig. 2). As all ion exchangers showed no significant uptake of Ca^{2+} the competitive measurements were carried out in the absence of Ca^{2+}. Both ion exchanger **1** and **2** are very selective for Cu^{2+}. The capacity of ion exchanger **1** for Cu^{2+} is high and constant over the whole pH range tested. The capacity of ion exchanger **2** for Cu^{2+} is much more pH dependent. At pH 1 a ligand occupation of 2% is achieved while at pH 5 the ligand occupation is over 40%. Ion exchanger **3** is selective for Cu^{2+} at lower pH <3 but at pH 5.5 the Cu^{2+} to Zn^{2+} ratio is only 2:1. The high Zn^{2+} uptake can be explained by assuming tridentate coordination of BBPAH. The coordination of Zn^{2+} through an aminopropyl-bridged benzimidazole was found to be relatively stable in an earlier investigation,[17] thus relative strong coordination of the 3-benzimidazole group in BBPAH is expected also, which accounts for the high ligand occupation Zn^{2+} at higher pH.

The distribution coefficient as a function of pH

The distribution coefficient[21] (D) of the three ion exchangers for Cu^{2+} as a function of pH, in the presence of chloride and acetate ions is shown in Fig. 3. The stability of the complexes on ion exchanger **1** is not dramatically influenced by changes in pH indicating that very strong Cu^{2+} complexes with BBAH are formed on the ion exchanger. Crystal structures of BBAH with copper(II) chloride show coordination of the Cu^{2+} ion in

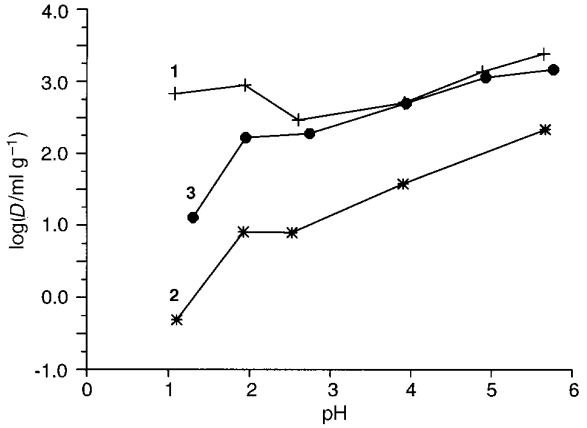

Fig. 3 Distribution coefficient (D) for Cu^{2+} as a function of pH for the ion exchangers **1**, **2** and **3**

a distorted square-pyramidal geometry.[22] In the equatorial plane the Cu^{2+} ion is coordinated by the three N-donors of BBAH and one chloride anion and a chloride anion in the axial position. This favourable geometry explains the high stability of the complexes on ion exchanger **1** and thereby its insensitivity towards acid.

The log D values for ion exchanger **2** are lower than in the other cases, which is consistent with the lower ligand occupation found in the metal-uptake experiments. The log D values of ion exchanger **2** have been compared with the values of the ligand aminoethylbenzimidazole which we investigated earlier,[17] and were found to be somewhat lower but follow the same trend. The difference might be caused by steric hindrance of the bulky benzimidazole moieties upon coordination to the metal ion. Unfortunately, only crystal structures with *N*,*N*′-bis(1-methylbenzimidazol-2-ylethyl)amine (MBBEAH) copper salts are known in the literature.[23] These show MBBEAH coordinating in a tridentate fashion *via* the 3N-donors of the ligand towards the Cu^{2+} ion. In case of perchlorate anions, a five-coordinate trigonal-bipyramidal geometry is found.[23]

The stability of the complexes formed on ion exchanger **3** is more dependent on pH than in the case of BBAH. The crystal structure of BBPAH with copper(II) chloride, $[Cu(BBPAH)(EtOH)(Cl)]_nCl_n$, consists of a polymeric structure in which a Cu^{2+} ion is coordinated in a square-pyramidal geometry. These findings suggest that absorption of Cu^{2+} on ion exchanger **3** is primarily through didentate binding of the ligand by the amine nitrogen and the 1-benzimidazole nitrogen *via* a five-membered metal–ligand chelate structure.

Description of the crystal structures with the ligand BBPAH

Reaction of BBPAH with $CuCl_2$ in ethanol resulted in the formation of the polymeric complex $[Cu(BBPAH)(EtOH)(Cl)]_nCl_n{\cdot}(n/2)EtOH$ (Fig. 4). A detailed three-dimensional structural analysis of the complex $[Cu(BBPAH)(EtOH)(Cl)]_nCl_n{\cdot}(n/2(EtOH)$ shows that the copper ions are coordinated in a square-pyramidal geometry. In the equatorial plane the copper ion is coordinated by the amine nitrogen N(1), a benzimidazole nitrogen N(23) and the symmetry related benzimidazole nitrogen N(13)($\frac{1}{2}+x$, $\frac{1}{2}-y$, $-z$). The coordination sphere is completed by a chloride, and an ethanol oxygen. The polymeric structure is stabilised by hydrogen-bonding interactions with chloride anions in the crystal lattice. A number of additional hydrogen-bond interactions, also involving a lattice ethanol, join the polymer into a two-dimensional framework in the *ab*-plane. Selected bond lengths and angles are listed in Table 3.

Reaction of BBPAH with $Ni(NO_3)_2$ in ethanol resulted in the formation of $[Ni(BBPAH)(H_2O)(NO_3)]NO_3{\cdot}2EtOH$ (Fig. 5). Structural analysis of this compound shows the nickel ion coordinated in an octahedral fashion by the amine nitrogen N(1), the benzimidazole nitrogen N(13) and the benzimidazole nitrogen N(23). The coordination sphere is completed by a water molecule and a didentate coordinated nitrate anion. Intermolecular hydrogen bonds and N—H···π interactions result in a three-dimensional framework comprising the Ni complex, a non-coordinating nitrate anion and two ethanol lattice molecules. Selected bond lengths and angles are listed in Table 4.

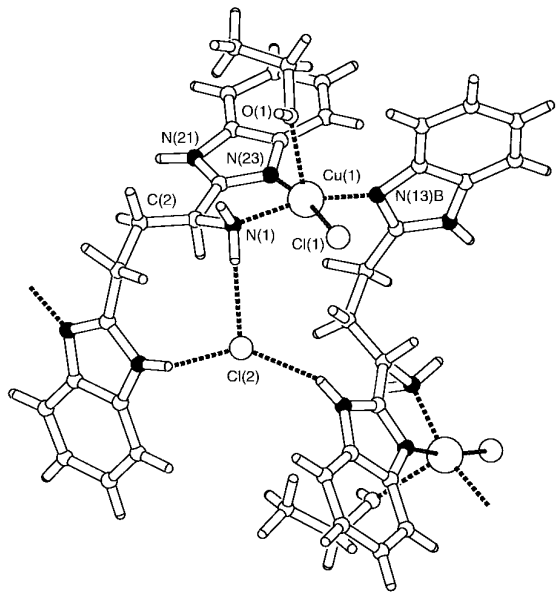

Fig. 4 PLUTON[25] plot of $[Cu(BBPAH)(EtOH)(Cl)]_nCl_n{\cdot}(n/2)$-$C_2H_6O$. Suffix B denotes symmetry operation $1/2+x$, $1/2-y$, $-z$. The minor disorder component of C(2) and the disordered solvent molecules have been omitted for clarity.

Table 3 Selected bond lengths (Å) and angles (°) for $[Cu(BBPAH)(EtOH)(Cl)]_nCl_n{\cdot}(n/2)EtOH$

Cu(1)–Cl(1)	2.277(2)	Cu(1)–N(23)	1.982(7)
Cu(1)–O(1)	2.323(6)	Cu(1)–N(13)B	1.961(6)
Cu(1)–N(1)	2.001(7)		
Cl(1)–Cu(1)–O(1)	96.93(16)	O(1)–Cu(1)–N(23)	87.6(2)
Cl(1)–Cu(1)–N(1)	90.9(2)	O(1)–Cu(1)–N(13)B	104.4(2)
Cl(1)–Cu(1)–N(23)	171.8(2)	N(1)–Cu(1)–N(23)	82.1(3)
Cl(1)–Cu(1)–N(13)B	90.17(18)	N(1)–Cu(1)–N(13)B	162.4(3)
O(1)–Cu(1)–N(1)	92.9(2)	N(23)–Cu(1)–N(13)B	95.3(3)

Suffix B denotes symmetry operation $\frac{1}{2}+x$, $\frac{1}{2}-y$, $-z$.

Uptake and regeneration of the ion exchangers

Data are listed in Table 5. Uptake of Cu^{2+} is fast for all three ion exchangers with an average $t_{\frac{1}{2}}$ of 30 s (the half-lives are estimated from the obtained uptake and stripping curves). Regeneration is also fast for ion exchangers **2** and **3** with 0.5 M H_2SO_4, but for ion exchanger **1**, 1 M H_2SO_4 was used and initial Cu^{2+} release is quite fast ($t_{\frac{1}{2}}$ of 10 s), but complete removal of Cu^{2+} takes much longer (up to 1 h). Slow regeneration is also seen in regeneration cycles (Table 6). Regeneration of ion exchanger **1** is performed with more concentrated acid compared to ion exchangers **2** and **3**. In contrast to **3**, the capacity of **1** and **2** is reduced after several cycles of loading and regeneration. Some additional tests were performed by shaking 0.2 g of ion exchangers **1** and **2** in demineralised water, or in dilute acid, for seven days. The elemental analysis data

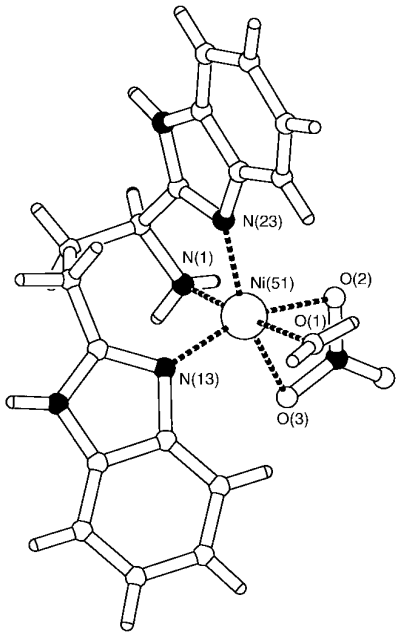

Fig. 5 PLUTON[25] plot of $[Ni(BBPAH)(H_2O)(NO_3)]\cdot NO_3\cdot 2EtOH$. Solvent molecules and the non-coordinated NO_3 anion have been omitted for clarity.

Table 4 Selected bond lengths (Å) and angles (°) for $[Ni(BBPAH)(H_2O)(NO_3)]NO_3\cdot 2EtOH$

Ni(51)–O(1)	2.028(6)	Ni(51)–N(1)	2.075(8)
Ni(51)–O(2)	2.147(6)	Ni(51)–N(13)	2.023(7)
Ni(51)–O(3)	2.181(5)	Ni(51)–N(23)	2.012(7)
O(1)–Ni(51)–O(2)	83.9(2)	O(2)–Ni(51)–N(23)	100.2(2)
O(1)–Ni(51)–O(3)	88.0(2)	O(3)–Ni(51)–N(1)	89.3(2)
O(1)–Ni(51)–N(1)	173.7(3)	O(3)–Ni(51)–N(13)	99.4(2)
O(1)–Ni(51)–N(13)	95.2(3)	O(3)–Ni(51)–N(23)	157.6(3)
O(1)–Ni(51)–N(23)	99.2(3)	N(1)–Ni(51)–N(13)	90.9(3)
O(2)–Ni(51)–O(3)	59.3(2)	N(1)–Ni(51)–N(23)	81.3(3)
O(2)–Ni(51)–N(1)	89.8(3)	N(13)–Ni(51)–N(23)	101.0(3)
O(2)–Ni(51)–N(13)	158.7(2)		

Table 5 Half-life data for Cu^{2+} uptake and stripping for ion exchangers **1**, **2** and **3**

ion exchanger	$t_{1/2}$ (uptake)/s	$t_{1/2}$ (stripping)/s
1	30	10[a]
2	30	10[b]
3	15	<10[b]

[a]1 M H_2SO_4. [b]0.5 M H_2SO_4.

are listed in Table 7. The results show that abrasive forces are not responsible for the reduction in ligand concentration. Therefore hydrolytic cleavage of surface or ligand bonds may be liable for this reduction and might also influence the kinetic data for these ion exchangers. The uptake and regeneration kinetics of polymer-immobilised BBAH and BBPAH are much slower as a consequence of the more hydrophobic nature of the polymers and the much larger particle size, but the ion exchangers are more stable towards hydrolysis. However, the difficulties in regenerating immobilised BBAH (polymer or silica) indicate that the kinetics are also strongly influenced by the structure of the ligands.

The Cu^{2+}–Zn^{2+} kinetic experiments under competitive conditions (Fig. 6), show that ion exchangers **2** and **3** have only a moderate selectivity towards Cu^{2+}, whilst ion exchanger **1** shows a much higher affinity for Cu^{2+}. Ion exchanger **2** also

Table 6 Cu^{2+} capacities (mmol Cu^{2+}/g ion exchanger) after several cycles of consecutive loading (24 h with $CuCl_2$ standard solution, NaOAc–HOAc buffer pH 4.5) and stripping (24 h with 1 M/0.5 M H_2SO_4)

cycle		**1**[a]	**2**[b]	**3**[b]
1	loaded	0.53	0.31	0.44
	stripped	0.01	<0.005	<0.005
2	loaded	0.52	0.27	0.49
	stripped	0.01	<0.005	<0.005
3	loaded	0.44	0.25	0.53
	stripped	0.01	<0.005	<0.005
4	loaded	0.38	0.22	0.52
	stripped	<0.005	<0.005	<0.005
5	loaded	0.33		0.49

[a]Stripping with 1 M H_2SO_4. [b]Stripping with 0.5 M H_2SO_4.

Table 7 Elemental analysis and ligand concentrations of the silica products

ion exchanger	%C	%H	%N	ligand conc./ mmol g^{-1}
1[a]	17.5	2.5	3.7	0.53
1 (blank)[b]	17.1	2.3	3.7	0.53
1 (2 M H_2SO_4)[c]	15.1	2.3	3.2	0.46
2	24.6	3.0	4.6	0.66
2 (blank)[b]	22.4	3.1	4.1	0.58
2 (0.1 M H_2SO_4)[c]	17.8	2.8	2.8	0.40
2 (0.5 M H_2SO_4)[c]	16.8	2.7	2.6	0.38
2 (2 M H_2SO_4)[c]	16.8	2.8	2.8	0.40

[a]From Table 2. [b]0.2 g ion exchanger was shaken in 50 ml demineralised water for seven days. [c]0.2 g ion exchanger was shaken in 50 ml acid for seven days.

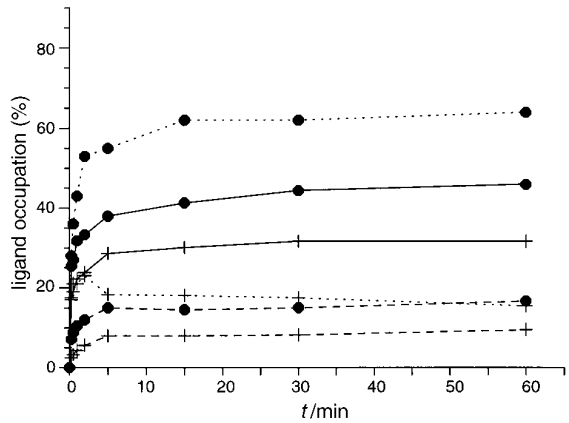

Fig. 6 Cu^{2+} and Zn^{2+} uptake under competitive conditions (1:1 mixture Cu^{2+}–Zn^{2+}, standard solution pH 5.0) for ion exchangers **1**, **2** and **3** [● Cu^{2+}, + Zn^{2+}; ··· **1**, −−− **2**, — **3**]

shows a much lower ligand occupation for Cu^{2+} and Zn^{2+} compared to **1** and **3**.

Spectroscopic data of the loaded samples and the coordination compounds

Data are listed in Table 8. The EPR data for $CuCl_2$-loaded **1** are suggestive of a tetragonally distorted square-pyramidal environment, with the three N-donor atoms of BBAH in the equatorial plane as found in several crystal structures. The coordination sphere is completed by chloride and/or acetate anion and water molecules. The LF spectrum shows a strong absorption maximum at 14.6×10^3 cm^{-1} which is very similar to that reported by Palaniandavar *et al.*[24] and is in agreement with the above described structure. The LF data of $NiCl_2$

Table 8 EPR and ligand field (LF) spectroscopic data for Cu^{2+}-loaded samples (loading: $CuCl_2$ standard solution, NaOAc–HOAc buffer pH 5.7)

sample	LF maxima $\nu/10^3$ cm^{-1}	EPR parameters		
		$g_\perp$	$g_{\|\|}$	$A_{\|\|}/G$
1 + $CuCl_2$	14.8	2.10	2.24	112
BBAH + $CuCl_2$ [a]	14.6			
1 + $NiCl_2$	27.0, 16.1, 9.9			
1 + $CoCl_2$	18.8, 12.1, 6.3			
2 + $CuCl_2$	14.1	2.08	2.28	118
2 + $NiCl_2$	25.8, 16.1, 9.0			
2 + $CoCl_2$	18.7, 8.5			
3 + $CuCl_2$	14.3	2.11	2.26	128
BBPAH + $CuCl_2$	15.8	2.07	2.20	
3 + $NiCl_2$	27.7, 16.5, 10			
BBPAH + $NiCl_2$	25.3, 13.6, 8.7			
3 + $CoCl_2$	17.3, 7.2			

[a]Ref. 11.

loaded **1** are consistent with a distorted octahedral geometry of a N_3X_3 chromophore (X = Cl, O). $CoCl_2$-loaded **1** suggests five-coordination by a N_3X_2 chromophore (X = Cl, O). Ion exchanger **2** loaded with $CuCl_2$ shows an absorption maximum at 14.1×10^3 cm^{-1} in the LF spectrum. Both the LF spectrum and the EPR data indicate tridentate coordination of BBEAH towards Cu^{2+}. The LF spectrum of the $NiCl_2$-loaded ion exchanger **2** is indicative of octahedral coordination by BBEAH. The EPR spectrum of $[Cu(BBPAH)(EtOH)(Cl)]_nCl_n$, is axial with $g_\perp = 2.08$ and $g_\parallel = 2.20$ and no hyperfine splitting is observed even at 77 K. A strong absorption at 15.8×10^3 cm^{-1} is seen in the LF spectrum. $CuCl_2$-loaded **3** however, shows hyperfine splitting and a LF maximum at 14.3×10^3 cm^{-1}. This is indicative of a N_3X_2 chromophore (X = Cl, O) with the 3-benzimidazole of BBPAH probably weakly coordinated in an axial position. The LF spectrum of $NiCl_2$-loaded **3** is in accord with a Ni^{2+} ion coordinated in an octahedral geometry in a tridentate fashion by the 3 nitrogen donors of the ligand.

Conclusion

The use of tridentate N-donor ligands, as described in the present paper, has shown that selectivity towards Cu^{2+} is comparable to the results which were achieved with the didentate analogs.[17] Alfa-BBAH shows strong binding of Cu^{2+}, even at low pH, as a consequence of the formation of very stable five-membered chelate complexes with the metal ion. The metal uptake of Alfa-BBEAH is much more dependent on pH, but only moderate ligand occupations are achieved. Alfa-BBPAH appears to coordinate strongly *via* a five-membered chelate, while the second benzimidazole is more weakly coordinated. This coordination mode was also observed in the crystal structure of BBPAH with $CuCl_2$ which was found to be polymeric, with one molecule of BBPAH chelating didentately to a Cu^{2+} ion and coordinating monodentately through the second benzimidazole group to a second Cu^{2+} ion.

The hydrolytic stability of the different silica-based ion exchangers was found to vary throughout this research, and no clear correlation with the ligand structure could be established. The choice of the base material will depend on the application. When mechanical stability is not too important a factor, ion exchangers based on organic polymers have the advantage of a higher hydrolytic stability and often a much higher ligand concentration than with the silica-based ion exchangers, although the kinetics are much slower.

Mr. F. Lefèber and Mr. J. G. Hollander are gratefully acknowledged for the collection of the solid-state CP MAS ^{13}C NMR spectra of the silica samples presented here. The work described in this paper was supported by the Leiden Study group WFMO (Werkgroep Fundamenteel Materialen Onderzoek) and in part (A.L.S., N.V.) by the Netherlands Foundation of Chemical Research (SON) with financial aid from the Netherlands Organisation for Scientific Research (NWO). Part of this work has been sponsored by the Ministry of Economical Affairs, the Ministry of Housing, Physical Planning and Environment and Senter I.O.P. Environmental Technology.

References

1 M. A. Grieg and D. Lindsay, *Ion Exchange for Industry*, ed. M. Streat, Ellis Horwood Limited, Chichester, 1988, p. 337.
2 J. T. M. Sluys, H. W. Bakkenes, R. J. M. Creusen, L. H. J. M. Schneiders and J. H. Hanemaaijer in *Membrane Processes in Separation and Purification*, ed. J. G. Crespo and K. W. Böddeker, NATO ASI series E, Kluwer, Dordrecht, 1994, vol. 272.
3 J. E. Cross and E. W. Hooper, *Ion Exchange for Industry*, ed. M. Streat, Ellis Horwood Limited, Chichester, 1988, p. 457.
4 S. K. Sahni and J. Reedijk, *Coord. Chem. Rev.*, 1984, **59**, 1.
5 S. K. Sahni, W. L. Driessen and J. Reedijk, *Inorg. Chim. Acta*, 1988, **154**, 141.
6 M. C. Millot, B. Sebille, A. Halli, H. Hommel and A. P. Legrand, *Chromatographia*, 1993, **37**, 584.
7 D. E. Leyden and G. H. Luttrell, *Anal. Chem.*, 1975, **47**, 584.
8 V. I. Fadeeva, T. I. Tikhomirova, I. B. Yuferova and G. V. Kudryavtsev, *Anal. Chim. Acta*, 1989, **219**, 201.
9 S. H. Chang, K. M. Gooding and F. E. Regnier, *J. Chromatogr.*, 1976, **120**, 321.
10 K. K. Unger, *Porous silica, Its Properties and use as a Support in Column Liquid Chromatography*, Journal of Chromatography Library Vol. 16, Elsevier Scientific, New York, 1979.
11 P. D. Verweÿ, T. Dugué, W. L. Driessen, J. Reedijk and D. C. Sherrington, *React. Polym.*, 1991, **14**, 213.
12 (*a*) P. M. van Berkel, D. J. Dijkstra, W. L. Driessen, J. Reedijk and D. C. Sherrington, *React. Funct. Polym.*, 1995, **28**, 39; (*b*) H. P. Berends and D. W. Stephan, *Inorg. Chim. Acta*, 1984, **93**, 73; (*c*) J. D. Crane and D. E. Fenton, *Polyhedron*, 1991, **10**, 1809.
13 T. N. Sorrell and M. L. Garrity, *Inorg. Chem.*, 1991, **30**, 210.
14 P. T. Beurskens, G. Admiraal, G. Beurskens, W. P. Bosman, S. García-Granda, R. O. Gould, J. M. M. Smits and C. Smykalla, The DIRDIF program system, Technical report of the Crystallographic Laboratory, University of Nijmegen, 1992.
15 G. M. Sheldrick, SHELXL-93, Program for crystal structure refinement, University of Göttingen, 1993.
16 N. Walker and D. Stuart, *Acta Crystallogr., Sect. A*, 1983, **39**, 158.
17 H. J. Hoorn, P. de Joode, W. L. Driessen and J. Reedijk, *React. Funct. Polym.*, 1995, **27**, 223.
18 K. Albert and E. Bayer, *J. Chromatogr.*, 1991, **544**, 345.
19 H. O. Kalinowski, S. Berger and S. Braun, *13C-NMR-Spektroskopie*, Georg Thieme Verlag, Stuttgart, 1984.
20 N. N. Greenwood and A. Earnshaw, *Chemistry of the Elements*, Pergamon Press, Oxford, 1984.
21 M. J. Hudson, in *Ion Exchange: Science and Technology*, ed. A. E. Rodrigues, Martinus Nijhoff, Dordrecht, 1986.
22 (*a*) D. Wahnon, R. C. Hynes and J. Chin, *J. Chem. Soc., Chem. Commun.*, 1994, 1441, (*b*) Y. Nishida, K. Takahashi and S. Kida, *Mem. Fac. Sci., Kyushu Univ. Ser. C* 1982, 13(**2**), 343.
23 L. Casella, O. Carugo, M. Gullotti, S. Doldi and M. Frassoni, *Inorg. Chem.*, 1996, **35**, 1101.
24 M. Palaniandavar, T. Pandiyan, M. Lakshminarayanan and H. Manohar, *J. Chem. Soc., Dalton Trans.*, 1995, 455.
25 A. L. Spek, PLUTON, Program for molecular graphics, Utrecht University, 1996.

Paper 7/01131F; *Received* 25*th February*, 1997